Bioorganic & Medicinal Chemistry 19 (2011) 6735–6742

Contents lists available at SciVerse ScienceDirect

Bioorganic & Medicinal Chemistry

journal homepage: www.elsevier.com/locate/bmc

Small molecular CD4 mimics as HIV entry inhibitors

Tetsuo Narumi [a], Hiroshi Arai [a], Kazuhisa Yoshimura [b], Shigeyoshi Harada [b], Wataru Nomura [a], Shuzo Matsushita [b], Hirokazu Tamamura [a,*]

[a] Institute of Biomaterials and Bioengineering, Tokyo Medical and Dental University, Chiyoda-ku, Tokyo 101-0062, Japan
[b] Center for AIDS Research, Kumamoto University, Kumamoto 860-0811, Japan

ARTICLE INFO

Article history:
Received 5 August 2011
Revised 23 September 2011
Accepted 24 September 2011
Available online 29 September 2011

Keywords:
CD4 mimic
HIV entry
gp120-CD4 interaction
Phe43 cavity

ABSTRACT

Derivatives of CD4 mimics were designed and synthesized to interact with the conserved residues of the Phe43 cavity in gp120 to investigate their anti-HIV activity, cytotoxicity, and CD4 mimicry effects on conformational changes of gp120. Significant potency gains were made by installation of bulky hydrophobic groups into the piperidine moiety, resulting in discovery of a potent compound with a higher selective index and CD4 mimicry. The current study identified a novel lead compound **11** with significant anti-HIV activity and lower cytotoxicity than those of known CD4 mimics.

1. Introduction

The dynamic supramolecular mechanism of HIV cellular invasion has emerged as a key target for blocking HIV entry into host cells.[1] HIV entry begins with the interaction of a viral envelope glycoprotein gp120 and a cell surface protein CD4.[2] This triggers extensive conformational changes in gp120 exposing co-receptor binding domains and allowing the subsequent binding of gp120 to a co-receptor, CCR5[3]/CXCR4.[4] Following the viral attachment and co-receptor binding, gp41, another viral envelope glycoprotein mediates the fusion of the viral and cell membranes, thus completing the infection. Molecules interacting with each of these steps are potential candidates for anti-HIV-1 drugs. In particular, discovery and development of novel drugs that inhibit the viral attachment are required for blocking the HIV infection at an early stage.[5]

In 2005, small molecular CD4 mimics targeting the viral attachment were identified by an HIV syncytium formation assay and shown to bind within the Phe43 cavity, a highly conserved pocket on gp120,[6] which is a hydrophobic cavity occupied by the aromatic ring of Phe43 of CD4.[7] These molecules are comprised of three essential moieties: an aromatic ring, an oxalamide linker, and a piperidine ring (Fig. 1) and show micromolar order potency against diverse HIV-1 strains including laboratory and primary isolates. Furthermore, they possess the unique ability to induce the conformational changes in gp120 required for binding with soluble CD4.[8] Such CD4 mimicry can be an advantage for rendering the envelope more sensitive to neutralizing antibodies.[9] While such properties are promising for the development of HIV entry inhibitors and the use combinatorially with neutralizing antibodies, cytotoxicity is one of the drawbacks of CD4 mimics.

To date, we and others have performed structure–activity relationship (SAR) studies of CD4 mimics based on modifications of the aromatic ring, the oxalamide linker, and the piperidine moiety of CD4 mimics. In an initial survey of SAR studies of NBD-556 and NBD-557, Madani et al. revealed that potency (i.e., CD4 binding and mimicry) was highly sensitive to modifications of the aromatic ring, which is thought to bind in the Phe43 cavity of gp120 (Fig. 1). The CD4 mimic analogs (JRC-II-191) with a *para*-chloro-*meta*-fluorophenyl ring had significantly increased affinity for gp120.[10] Our SAR studies also revealed that a certain size and electron-withdrawing ability of the *para*-substituents are indispensable for potent anti-HIV activity.[11] Furthermore, the replacement of the chlorine group at the *para* position with a methyl group which is almost as bulky as a bromine atom leads to improvement of solubility of the compounds in buffer to provide the reproducibility in the biological studies with comparable biological activities.

Further SAR studies were focused on the piperidine moiety of CD4 mimics to investigate its contribution to biological activities, and we found that the piperidine ring is critical for the CD4 mimicry on the conformational changes in gp120 and that substituents on the nitrogen of the piperidine moiety can contribute significantly to both anti-HIV activity and cytotoxicity.[12] Based on these SARs and our modeling study, we speculate that interactions of the piperidine moiety with several amino acids in the vicinity of the Phe43 cavity in gp120, specifically an electrostatic interaction with

* Corresponding author. Tel.: +81 3 5280 8036; fax: +81 3 5280 8039.
E-mail address: tamamura.mr@tmd.ac.jp (H. Tamamura).

0968-0896/$ - see front matter © 2011 Elsevier Ltd. All rights reserved.
doi:10.1016/j.bmc.2011.09.045

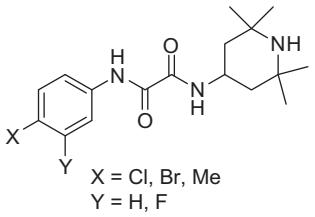

Figure 1. CD4 mimics.

Asp368 and a hydrophobic interaction with Val430, are critical for biological activity. LaLonde et al. focused on modifications of the piperidine moiety using computational approaches, adducing evidence for the importance of these interactions to the binding affinity against gp120.[13] Based on these results, we envisioned that an enhancement of the interaction of CD4 mimics with residues associated with the Phe43 cavity in gp120 would lead to the increase of their potency and CD4 mimicry inducing the conformational changes of gp120, and the decrease of their cytotoxicity. Thus, in this study a series of CD4 mimics, which were designed to interact with the conserved residues in the Phe43 cavity, were synthesized to increase binding affinity for gp120, and the appropriate SAR studies were performed.

2. Results and discussion

Two types of CD4 mimic analogs were designed: (1) CD4 mimics with the ability to interact electrostatically with Asp368, and (2) CD4 mimics with the ability to interact hydrophobically with Val430 (Fig. 2). The X-ray structure of gp120 bound to soluble CD4 (PDB: 1RZJ) revealed that the guanidino group of Arg59 of CD4 is involved in a hydrogen bond with Asp368 of gp120. In order to mimic this interaction, a guanidino and related groups such as thiourea and urea were introduced to the piperidine moiety of the CD4 mimic derivative COC-021, which was developed in order to modify the nitrogen of the piperidine moiety and which showed biological activity, including anti-HIV activity and CD4 mimicry, similar to that of the parent compound NBD-556.[12] Furthermore, to interact with Val430 by hydrophobic interaction, the methyl groups on the piperidine ring were replaced with cyclohexyl groups to prepare a novel CD4 mimic analog with enhanced hydrophobicity.

2.1. Chemistry

The syntheses of CD4 mimics are outlined in Scheme 1. CD4 mimics with guanidine, thiourea, and urea groups on the piperidine moiety were prepared using our previously reported method.[12] Coupling of *p*-chloroaniline with ethyl chloroglyoxylate followed by aminolysis of the ethyl ester with 4-amino-*N*-benzylpiperidine under microwave conditions (150 °C, 3 h) gave the corresponding amide. Removal of the benzyl group with 1-chloroethyl chloroformate[14] gave the free piperidine moiety, which was modified to produce the desired compounds **4**–**8** (Scheme 1).

For synthesis of a CD4 mimic derivative with two cyclohexyl groups, treatment of 2,2,6,6-tetramethylpiperidin-4-one **9** with cyclohexanone in the presence of ammonium chloride furnished a 2,6-substituted piperidin-4-one derivative,[15] and reductive amination with benzylamine and subsequent removal of benzyl group provided a primary amine **10**. Microwave-assisted aminolysis of ester **2** with amine **10** yielded the desired dicyclohexyl-substituted analog **11** (Scheme 2). The synthesis of the other compounds is described in Supplementary data.

2.2. Biological studies

The anti-HIV activity of synthetic CD4 mimics was evaluated in a single-round viral infective assay. Inhibition of HIV-1 infection was measured as reduction in β-galactosidase gene expression after a single-round of virus infection of TZM-bl cells as described previously.[9] IC_{50} was defined as the concentration that caused a 50% reduction in the β-galactosidase activity (relative light units [RLU]) compared to virus control wells. Cytotoxicity

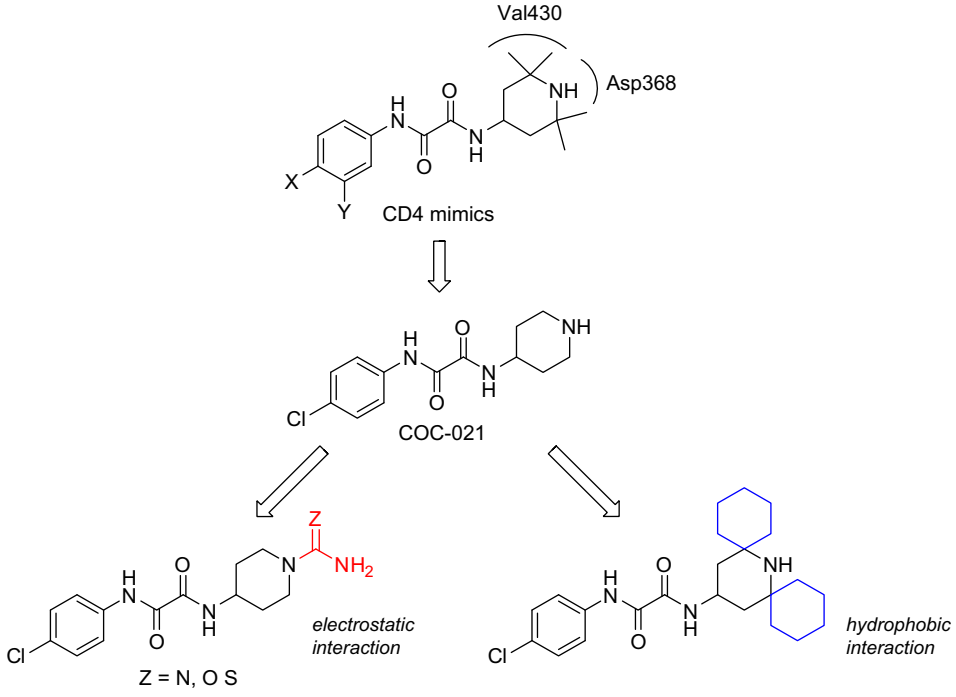

Figure 2. Design strategy for novel CD4 mimics with enhanced electrostatic/hydrophobic interaction.

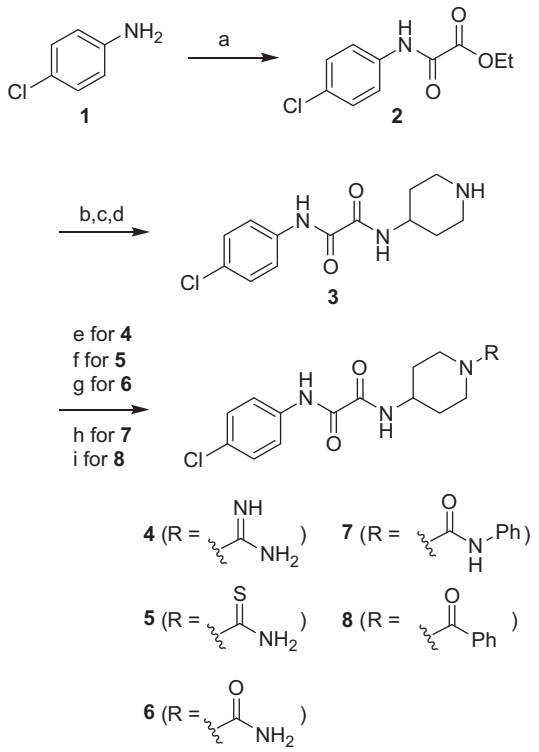

Scheme 1. Synthesis of N-modified piperidine derivatives **4**–**8**. Reagents and conditions: (a) Ethyl chloroglyoxylate, Et_3N, THF, quant.; (b) 1-benzyl-4-aminopiperidine, Et_3N, EtOH, 150 °C, microwave, 78%; (c) 1-chloroethyl chloroformate, CH_2Cl_2; (d) MeOH, reflux, 64% in two steps; (e) 1*H*-pyrazole-1-carboxamidine hydrochloride, Et_3N, DMF, 61%; (f) (trimethylsilyl)isothiocyanate, $CHCl_3$, 36%; (g) (trimethylsilyl)isocyanate, $CHCl_3$, 30%; (h) phenyl isocyanate, $CHCl_3$, 32%, (i) benzoyl chloride, Et_3N, CH_2Cl_2, 68%.

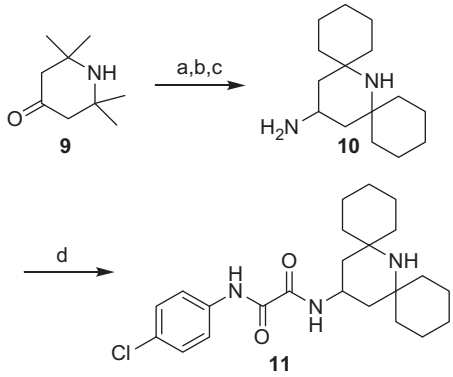

Scheme 2. Synthesis of dicyclohexyl derivative **11**. Reagents and conditions: (a) Cyclohexanone, NH_4Cl, DMSO, 60 °C; (b) benzylamine, $NaBH_4$, MeOH; (c) 10% Pd/C, H_2, MeOH, 7% from **9**; (d) **2**, Et_3N, EtOH, 150 °C, microwave, 17%.

of the compounds based on the viability of mock-infected PM1/CCR5 cells was evaluated using WST-8 method. The assay results for the CD4 mimics **3**–**8** are shown in Table 1. Compound **12** (NBD-556) showed potent anti-HIV activity; its IC_{50} value was 0.61 μM, and it is thus 13–20-fold more potent than the reported values.[11,12] Although previous studies found that compound **13**, with a methyl group at the *p*-position of the phenyl ring, and compound **3**, with no dimethyl groups on the piperidine ring, showed potent anti-HIV activity, only moderate activities were observed in the current study; this is about 12–14-fold less potency than reported for compound **12** and is probably due to

Table 1
Effects of the nitrogen-substituents on anti-HIV activity and cytotoxicity of CD4 mimic analogs[a]

Compd	X	R	IC_{50}[b] (μM)	CC_{50}[c] (μM)	SI (CC_{50}/IC_{50})
		YTA (R5)			
3[d]	Cl	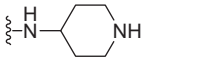	7.0	51	7.3
4[e]	Cl	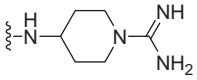	6.1	72	12
5	Cl	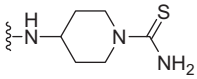	5.5	42	7.6
6	Cl	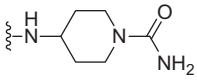	8.3	310	37
7	Cl	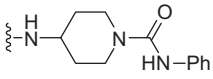	11	6.2	0.56
8	Cl	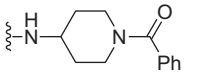	5.1	ND	—
12 (NBD-556)	Cl	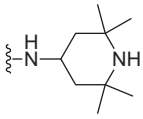	0.61	35	57
13	Me	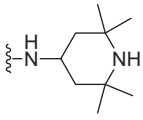	8.4	260	31

[a] All data with standard deviation are the mean values for at least three independent experiments (ND = not determined)
[b] IC_{50} values are based on the reduction in the β-galactosidase activity in TZM-bl cells.
[c] CC_{50} values are based on the reduction of the viability of mock-infected PM1/CCR5 cells.
[d] Desalted by satd $NaHCO_3$ aq.
[e] TFA salts.

the different assay system. All of the synthesized novel derivatives of compound **12** showed moderate to potent anti-HIV activity. A guanidine derivative **4** and thiourea derivative **5** showed potent anti-HIV activities (IC_{50} of **4** = 6.1 μM and IC_{50} of **5** = 5.5 μM) but their potency was approximately 10-fold lower than that of the parent compound **12**. A urea derivative **6** also showed potent anti-HIV activity (IC_{50} = 8.3 μM) and exhibited lower cytotoxicity (CC_{50} = 310 μM). On the other hand, introduction of a phenyl group in the urea derivative **6**, led to an *N*-phenylurea derivative **7**, with an increase of cytotoxicity (CC_{50} = 6.2 μM). To examine the influence of the N–H group on anti-HIV activity, an *N*-benzoyl derivative **8** was also tested. The IC_{50} value of **8** was 5.1 μM, which is equipotent with the thioamide derivative **5**. The *N*-benzoyl derivative **8** was essentially equipotent with **3** and this result suggests the presence of the hydrogen atom of the N–H group does not contribute to an increase in anti-HIV activity. The thiourea derivative **5** and the *N*-phenylurea derivative **7**, which have more acidic protons (pK_a of thiourea and *N*-phenylurea; 21.0 and 19.5,[16] respectively) than the urea derivative **6** (pK_a of urea; 26.9[16]), were found to exhibit relatively strong cytotoxicity. This observation indicates that

Table 2
Anti-HIV activity and cytotoxicity of CD4 mimic analogs **11**, **12**, and **14–17**[a]

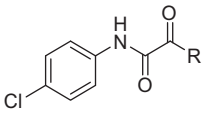

Compd	R	YTA (R5) IC$_{50}$[b] (μM)	CC$_{50}$[c] (μM)	SI (CC$_{50}$/IC$_{50}$)
11	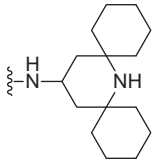	0.68	120	176
14	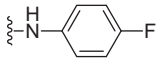	3.1	>500	>160
15	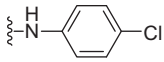	>100	>500	—
16	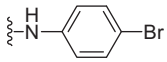	>100	>500	—
17	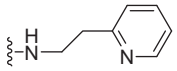	19.8	480	24
12 (NBD-556)	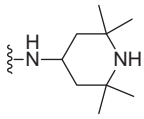	0.61	35	57

[a] All data with standard deviation are the mean values for at least three independent experiments
[b] IC$_{50}$ values are based on the reduction in the β-galactosidase activity in TZM-bl cells.
[c] CC$_{50}$ values are based on the reduction of the viability of mock-infected PM1/CCR5 cells.

Table 3
Anti-HIV activity of CD4 mimic **12** and dicyclohexyl derivative **11**[a]

Compd	R	IC$_{50}$[b] (μM) Single-round assay	IC$_{50}$[c] (μM) Multi-round assay
12 (NBD-556)	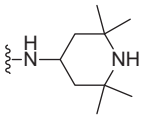	0.61	0.90
11	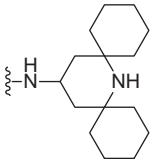	0.68	0.56

[a] All data with standard deviation are the mean values for at least three independent experiments.
[b] IC$_{50}$ values of the single-round assay are based on the reduction in the β-galactosidase activity in TZM-bl cells.
[c] IC$_{50}$ values of the multi-round assay are based on the inhibition of HIV-1-induced cytopathogenicity in PM1/CCR5 cells.

substitution on the piperidine moiety of acidic functional groups was unfavorable.

The assay results for CD4 mimics that target hydrophobic interactions are shown in Table 2. Compound **11** showed significant anti-HIV activity (IC$_{50}$ = 0.68 μM) comparable to that of the lead compound **12**, but exhibited lower cytotoxicity. Compound **11** showed approximately four-fold less cytotoxicity than **12**. The SI of **11** is 176, 3 times higher than that of **12** (SI = 57). This result suggests that substitution of bulky hydrophobic groups into the piperidine moiety may be consistent with lower cytotoxicity of CD4 mimics. It is noteworthy that compound **14**, which has a *p*-fluoroanilino group in place of the piperidine ring, exhibits potent anti-HIV activity (IC$_{50}$ = 3.1 μM) without significant cytotoxicity (CC$_{50}$ >500 μM). The SI of compound **14** is >160, which is comparable to that of **11**. However, replacement of the piperidine moiety with a *p*-bromo- or *p*-chloroanilino group resulted in the loss of anti-HIV activity. These results suggest that the introduction of a fluorine atom to the piperidine moiety might be consistent with improvement of the anti-HIV activity. Extension of the alkyl chain by two carbons, as in **17** resulted in a 30-fold loss of anti-HIV activity, indicating that relatively rigid structures are preferable for anti-HIV activity.

The anti-HIV activities of **12** and compound **11**, which has a higher SI than the parent compound **12** were evaluated in a multi-round viral infective assay and the results are shown in Table 3. In this assay, the IC$_{50}$ value of **12** was 0.90 μM, which was slightly larger value than measured in a single-round assay (IC$_{50}$ = 0.61 μM). Compound **11** showed higher anti-HIV activity (IC$_{50}$ = 0.56 μM) than compound **12**, indicating that the introduction of hydrophobic cyclohexyl groups into the piperdine moiety has a positive effect on not only the cytotoxicity but also the anti-HIV activity. This is possibly due to the stability in the assay condition derived from the hydrophobicity of cyclohexyl group(s). These results are consistent with a previous study of the analog with one hydrophobic *gem*-dimethyl group on the piperidine moiety, a compound with potent anti-HIV activity and efficient binding affinity for gp120.[13]

To gain insight into the interactions involved in the binding, molecular modeling of compound **11** docked into gp120 (1RZJ) was carried with Sybyl 7.1 (Fig. 3). The binding mode of compound **11** in the Phe43 cavity suggested that the orientation of the piperidine moiety of **11** is different from that in compound **12**, and that the cyclohexyl group can be positioned near Val430 with whose isopropyl group it can interact hydrophobically.

Fluorescence activated cell sorting (FACS) analysis was performed as previously reported,[11,12] to evaluate the CD4 mimicry effects on conformational changes of gp120 and the results are shown in Figure 4. Comparison of the binding of an anti-envelope CD4-induced monoclonal antibody (4C11) to the cell surface pretreated with the above CD4 mimics was measured in terms of the mean fluorescence intensity (MFI). Our previous studies revealed that the profile of the binding of 4C11 to the Env-expressing cell surface pretreated with compound **12** was entirely similar to that of pretreatment of soluble CD4. In this FACS analysis, the MFI of pretreatment with compound **12** is 23.13. The profiles of the binding of 4C11 to the cell surface pretreated with compounds **3**, **4** and **5** were comparable to that of compound **12** [MFI (**3**) = 20.54**,** MFI (**4**) = 20.85**,** MFI (**5**) = 20.24, respectively], suggesting that these derivatives offer a significant enhancement of binding affinity for 4C11. On the other hand, pretreatment with **6** and **8** did not cause significant enhancement of the binding affinity for 4C11, indicating that introduction of a carbonyl group on the piperidine nitrogen is not conducive to CD4 mimicry. The profile of the binding of 4C11 to the Env-expressing cell surface pretreated with compound **11**, which had significant anti-HIV activity and lower cytotoxicity than compound **12**, (MFI (**11**) = 22.17) was similar to that of compound **12**, suggesting that compound **11** offers significant enhancement of binding affinity for 4C11. This result indicates that compound **11** retains the CD4 mimicry on the conformational changes of gp120. Although compound **14** and compound **17** showed potent anti-HIV activity and no significant cytotoxicity, the profiles pretreated with (MFI (**14** and **17**) = 15.20 and 15.38) were similar to that of the control (MFI = 14.94), suggesting that these compounds **14** and **17** failed to produce a significant increase in binding affinity for 4C11. These

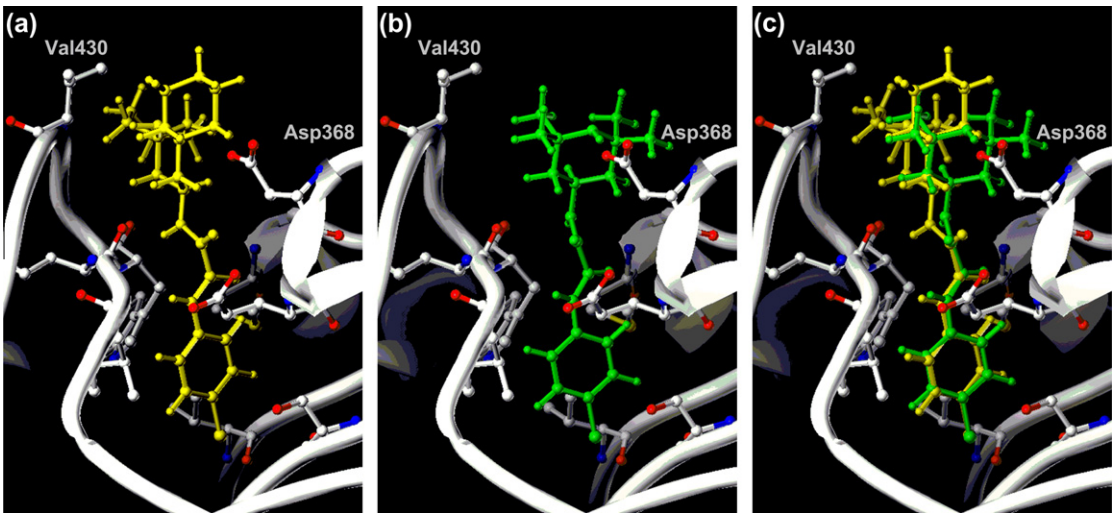

Figure 3. Docking structures of (a) compound **11** and (b) compound **12** bound in the Phe43 cavity of gp120 (1RZJ); (c) merge image of compounds **11** and **12**. Compounds **11** and **12** are represented in yellow and green sticks, respectively. Key residues in the cavity forming interactions with compounds are represented in gray sticks.

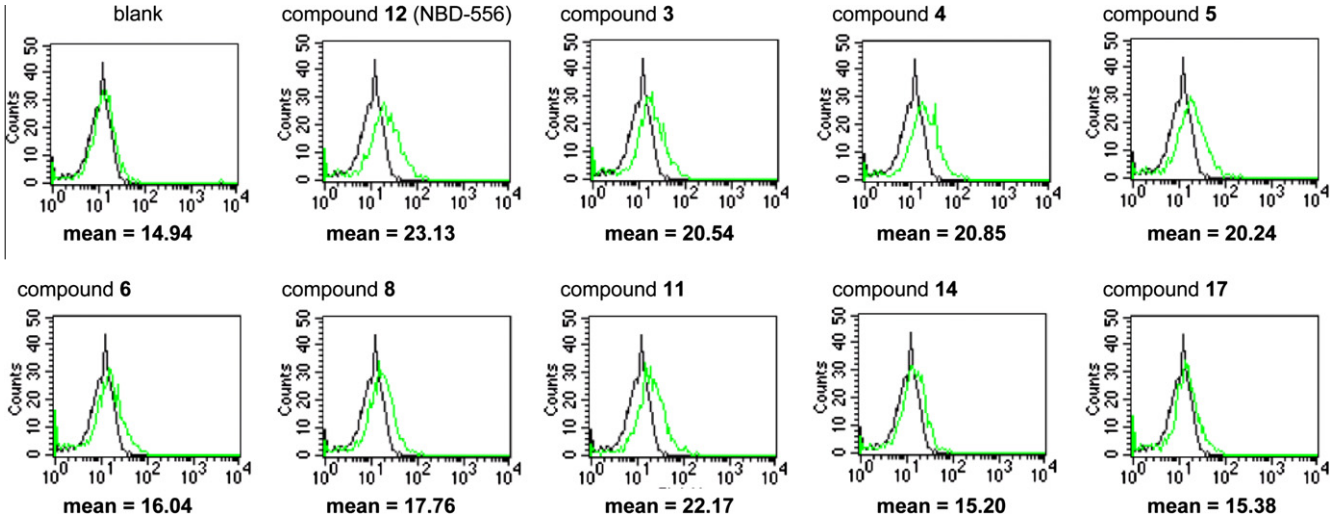

Figure 4. FACS analysis of compounds **12**, **3**–**6**, **8** (Table 1), **11**, **14**, and **17** (Table 2).

results are consistent with our previous finding that the piperidine ring is critical to the CD4 mimicry of the conformational changes in gp120.

3. Conclusion

A series of CD4 mimics were designed and synthesized to interact with the conserved residues in the Phe43 cavity of gp120 to investigate their anti-HIV activity, cytotoxicity, and CD4 mimicry as a function of conformational change of gp120. The biological activities of the synthetic compounds indicate that (1) the hydrogen atom of the piperidine moieties contributes significantly to cytotoxicity, and (2) installation of bulky hydrophobic groups into the piperidine moiety can increase anti-HIV activity and decrease cytotoxicity thus providing a novel compound with higher selective index than those of the original CD4 mimics. Furthermore, this modification has no great influence on the CD4 mimicry on the conformational change of gp120. Thus, compound **11** is promising for further studies. More detailed SAR investigations with respect to the substitution on the piperidine moiety have been ongoing studies.

4. Experimentals

^{1}H NMR and ^{13}C NMR spectra were recorded using a Bruker Avance III spectrometer. Chemical shifts are reported in δ (ppm) relative to Me_4Si (in $CDCl_3$) as internal standard. Low- and high-resolution mass spectra were recorded on a Bruker Daltonics microTOF focus in the positive and negative detection mode. For flash chromatography, Wakogel C-200 (Wako Pure Chemical Industries, Ltd) and silica gel 60 N (Kanto Chemical Co., Inc.) were employed. For analytical HPLC, a Cosmosil $5C_{18}$-ARII column (4.6 × 250 mm, Nacalai Tesque, Inc., Kyoto, Japan) was employed with a linear gradient of CH_3CN containing 0.1% (v/v) TFA at a flow rate of 1 cm^3 min^{-1} on a JASCO PU-2089 plus (JASCO Corporation, Ltd., Tokyo, Japan), and eluting products were detected by UV at 220 nm. Preparative HPLC was performed using a Cosmosil $5C_{18}$-ARII column (20 × 250 mm, Nacalai Tesque, Inc.) on a JASCO PU-2087 plus (JASCO Corporation, Ltd, Tokyo, Japan) in a suitable

gradient mode of CH_3CN solution containing 0.1% (v/v) TFA at a flow rate of 7 cm^3 min^{-1}. Microwave reactions were performed in Biotage Microwave Reaction Kit (sealed vials) in an Initiator™ (Biotage). The wattage was automatically adjusted to maintain the desired temperature for the desired period of time.

4.1. Chemistry

4.1.1. N^1-(4-Chlorophenyl)-N^2-(piperidin-4-yl)oxalamide (3)

To a stirred solution of *p*-choroaniline (**1**) (14.0 g, 110 mmol) in THF (146 mL) were added ethyl chloroglyoxylate (8.13 mL, 73.2 mmol) and triethylamine (Et_3N) (15.2 mL, 110 mmol) at 0 °C. The mixture was stirred for 6 h at room temperature. After the precipitate was filtrated off, the filtrate solution was concentrated under reduced pressure. The residue was dissolve in EtOAc, and washed with 1 M HCl, saturated $NaHCO_3$ and brine, then dried over $MgSO_4$. Concentration under reduced pressure gave the crude ethyl oxalamate, which was used without further purification. To a solution of the above ethyl oxalamate (1.27 g, 5.25 mmol) in EtOH (13.0 mL) were added Et_3N (1.46 mL, 10.5 mmol) and 4-amino-1-benzylpiperidine (2.97 mL, 15.8 mmol). The reaction mixture was stirred for 3 h at 150 °C under microwave irradiation. After being cooled to room temperature, the crystal was collected and washed with cold EtOH and *n*-hexane, and dried under reduced pressure to provide the corresponding amide (1.58 g, 81% yield) as colorless crystals. To a stirred solution of **S1** (1.46 g, 3.90 mmol) in CH_2Cl_2 (39.0 mL) was added dropwise 1-chloroethyl chloroformate (0.860 mL, 7.80 mmol) at 0 °C. After being stirred at room temperature for 30 min, the mixture was refluxed for 1 h. After concentration under reduced pressure, the residue was dissolved in MeOH and then refluxed for 1 h. After concentration under reduced pressure, the residue was diluted with EtOAc and washed with saturated $NaHCO_3$ and brine, then dried over $MgSO_4$. After concentration under reduced pressure, the residue was washed with cold EtOAc, and dried under reduced pressure to provide the title compound **3** (778 mg, 71% yield) as white powder.

^{1}H NMR (400 MHz, $CDCl_3$) δ 1.39–1.52 (m, 2H), 1.92–2.01 (m, 2H), 2.67–2.79 (m, 2H), 3.06–3.19 (m, 2H), 3.83–3.95 (m, 1H), 7.34 (d, J = 8.80 Hz, 2H), 7.44 (d, J = 7.64 Hz, 1H), 7.59 (d, J = 8.80 Hz, 2H), 9.28 (s, 1H); ^{13}C NMR (125 MHz, $CDCl_3$) δ 33.0 (2C), 45.2 (2C), 47.9, 21.0 (2C), 129.3 (2C), 130.5, 135.0, 157.6, 158.8; HRMS (ESI), *m/z* calcd for $C_{13}H_{17}ClN_3O_2$ (MH^+) 282.1004, found 282.1002.

4.1.2. N^1-(1-Carbamimidoylpiperidin-4-yl)-N^2-(4-chlorophenyl) oxalamide (4)

To a stirred solution of **3** (50.0 mg, 0.178 mmol) in DMF (20.0 mL) was added 1-aminopyrazole hydrochlride (312 mg, 2.13 mmol) and Et_3N (0.390 mL, 28.1 mmol). The reaction mixture was stirred at room temperature for 24 h. After concentration under reduced pressure, purification by preparative HPLC gave the trifluoroacetate of the title compound **4** as white powder (36.0 mg, 61% yield).

^{1}H NMR (500 MHz, DMSO) δ 1.41–1.55 (m, 2H), 1.59–1.71 (m, 2H), 2.70–2.74 (m, 2H), 3.74–3.87 (m, 1H), 3.88–4.03 (m, 2H), 5.93 (s, 2H), 7.42 (d, J = 9.00 Hz, 2H), 7.85 (d, J = 9.00 Hz, 2H), 8.95 (d, J = 9.00 Hz, 1H), 10.80 (s, 1H); ^{13}C NMR (125 MHz, DMSO) δ 31.3 (2C), 43.0 (2C), 47.6, 122.4 (2C), 128.6, 129.1 (2C), 137.1, 158.2, 159.3, 159.5; HRMS (ESI), *m/z* calcd for $C_{14}H_{19}ClN_5O_2$ (MH^+) 324.1222, found 324.1213.

4.1.3. N^1-(1-Carbamothioylpiperidin-4-yl)-N^2-(4-chlorophenyl) oxalamide (5)

To a stirred solution of **3** (140 mg, 0.498 mmol) in $CHCl_3$ (5.00 mL) was added trimethylsilyl isothiocyanate (141 mL, 1.00 mmol) and stirred at room temperature for 1 h. The precipitate was collected and washed with cold $CHCl_3$, and dried under reduced pressure to provide the title compound **5** as white powder. (62.0 mg, 36% yield).

^{1}H NMR (400 MHz, DMSO) δ 1.45–1.69 (m, 2H), 1.69–1.81 (m, 2H), 2.67–2.81 (m, 2H), 3.02–3.16 (m, 2H), 3.75–3.89 (m, 1H), 7.41 (d, J = 9.00 Hz, 2H), 7.85 (d, J = 9.00 Hz, 2H), 9.00 (d, J = 8.50 Hz, 1H), 10.80 (s, 1H); ^{13}C NMR (125 MHz, DMSO) δ 27.8 (2C), 42.3 (2C), 44.4, 122.0 (2C), 128.2, 128.6 (2C), 129.5, 136.6, 158.6, 159.4; Anal. calcd for $C_{14}H_{18}ClN_4O_2S$: C, 49.34; H, 5.03; N, 16.44. Found: C, 49.32; H, 4.76; N, 16.11.

4.1.4. N^1-(1-Carbamoylpiperidin-4-yl)-N^2-(4-chlorophenyl) oxalamide (6)

To a stirred solution of **3** (60.0 mg, 0.213 mmol) in $CHCl_3$ (1.10 mL) was added trimethylsilyl isocyanate (56.0 μL, 0.421 mmol), and the mixture was stirred at room temperature for 1 h. The precipitate was collected and washed with cold $CHCl_3$, and dried under reduced pressure to provide the title compound **6** (20.1 mg, 30% yield) as white powder.

^{1}H NMR (500 MHz, DMSO) δ 1.44–1.55 (m, 2H), 1.58–1.71 (m, 2H), 2.65–2.78 (m, 2H), 3.76–3.87 (m, 1H), 3.87–4.01 (m, 2H), 5.94 (s, 1H), 7.42 (d, J = 9.00 Hz, 2H), 7.86 (d, J = 9.00 Hz, 2H), 8.95 (d, J = 9.00 Hz, 1H), 10.80 (s, 1H); ^{13}C NMR (125 MHz, DMSO) δ 30.8 (2C), 42.6 (2C), 47.1, 122.0 (2C), 128.1, 128.6 (2C), 136.7, 157.8, 158.8, 159.0; HRMS (ESI), *m/z* calcd for $C_{14}H_{18}ClN_4O_3$ (MH^+) 325.1062, found 325.1060.

4.1.5. N^1-(4-Chlorophenyl)-N^2-(1-(phenylcarbamoyl)piperidin-4-yl)oxalamide (7)

To a stirred solution of **3** (140 mg, 0.498 mmol) in $CHCl_3$ (5.00 mL) was added phenyl isocyanate (54.0 μL, 0.500 mmol) and stirred at room temperature for 1 h. The precipitate was collected and washed with cold $CHCl_3$, and dried under reduced pressure to provide the title compound **7** as white powder. (64.1 mg, 32% yield).

^{1}H NMR (500 MHz, DMSO) δ 1.52–1.66 (m, 2H), 1.68–1.80 (m, 2H), 2.81–2.95 (m, 2H), 3.84–3.96 (m, 1H), 4.08–4.20 (m, 2H), 6.91–6.94 (m, 2H), 7.21–7.24 (m, 2H), 7.36–7.52 (m, 4H), 7.86 (d, J = 9.00 Hz, 2H), 8.53 (s, 1H), 8.99 (d, J = 8.50 Hz, 2H), 10.81 (s, 1H); ^{13}C NMR (125 MHz, DMSO) δ 31.3 (2C), 43.4 (2C), 47.5, 120.0 (2C), 122.0, 122.4 (2C), 128.6, 128.7 (2C), 129.1 (2C), 137.1, 141.1, 155.2, 159.2, 159.5; HRMS (ESI), *m/z* calcd for $C_{20}H_{22}ClN_4O_3$ (MH^+) 401.1375, found 401.1372.

4.1.6. N^1-(1-Benzoylpiperidin-4-yl)-N^2-(4-chlorophenyl) oxalamide (8)

To a stirred solution of **3** (500 mg, 1.78 mmol) in $CHCl_3$ (17.8 mL) was added benzoyl chloride (307 μL, 2.67 mmol) and the mixture was stirred at room temperature for 1 h. The precipitate was collected and washed with cold EtOAc, and dried under reduced pressure to provide the title compound **8** (232 mg, 34% yield).

^{1}H NMR (500 MHz, $CDCl_3$) δ 1.21–1.68 (br, 4H), 1.96–2.08 (br, 2H), 3.02–3.16 (br, 2H), 4.04–4.07 (m, 1H), 7.35 (d, J = 9.00 Hz, 2H), 7.41–7.43 (m, 5H), 7.52 (d, J = 8.00 Hz, 1H), 7.59 (d, J = 9.00 Hz, 2H), 9.25 (s, 1H); ^{13}C NMR (125 MHz, $CDCl_3$) δ 31.4 (2C), 41.0 (2C), 47.6, 121.0 (2C), 126.9 (2C), 128.6 (2C), 129.3 (2C), 129.9, 130.6, 134.8, 135.6, 157.2, 159.0, 170.5; HRMS (ESI), *m/z* calcd for $C_{20}H_{21}ClN_3O_3$ (MH^+) 386.1266, found 386.1276.

4.1.7. Amine (10)

To a stirred solution of 2,2,6,6-tetramethylpiperidin-4-one (7.75 g, 50.0 mmol) and cyclohexanone (15.5 mL, 150 mmol) in DMSO (71.0 mL) was added NH_4Cl (16.1 g, 300 mmol) and stirred at 60 °C for 5 h. The reaction mixture was diluted with H_2O

(150 mL), acidified with 7% aq HCl, and extracted with Et_2O (200 mL × 3). The water layer was adjusted to pH 9 using 10% aq K_2CO_3 and then back-extracted with EtOAc. The extract was washed with brine and dried over Na_2SO_4. After concentration under reduced pressure, the residue was dissolve in MeOH (60.0 mL) and benzylamine (10.9 mL, 100 mmol) was added. After being stirred at room temperature for 1 h, sodium cyanoborohydride was added and stirred at room temperature for 6 h. The reaction mixture was poured into saturated $NaHCO_3$ and extracted with EtOAc, then dried over $MgSO_4$. After concentration under reduced pressure, the residue was dissolve in MeOH (150 mL) and 10% Pd/C (5.32 g, 5.00 mmol) was added and stirred at room temperature for 24 h under hydrogen atmosphere. After the reaction mixture was filtered through celite, the filtrate solution was concentrated under reduced pressure followed by flash chromatography over silica gel with EtOAc–EtOH (4:1) to gave the title compound **10** (820 mg, 7 % yield) as a colorless oil.

^{1}H NMR (500 MHz, $CDCl_3$) δ 0.730 (t, J = 12.0 Hz, 2H), 1.15–1.85 (m, 23H), 2.01–3.7 (m, 2H), 2.95–3.05 (m, 1H); ^{13}C NMR (125 MHz, $CDCl_3$) δ 22.2 (2C), 22.8 (2C), 26.2 (2C), 37.3 (2C), 42.3 (2C), 43.6 (2C), 47.0, 53.2 (2C); HRMS (ESI), *m/z* calcd for $C_{15}H_{29}N_2$ (MH^+) 237.2325, found 237.2321.

4.1.8. N^1-(4-Chlorophenyl)-N^2-(2,6-dicyclohexylpiperidin-4-yl) oxalamide (11)

To a solution of **10** (722 mg, 3.05 mmol) in EtOH (15.0 mL) was added ethyl 2-((4-chlorophenyl)amino)-2-oxoacetate (363 mg, 1.50 mmol) and triethylamine (0.415 mL, 3.00 mmol) and stirred for 3 h at 150 °C under microwave irradiation. The mixture was filtered and the precipitate was collected and washed with cold EtOH, and dried under reduced pressure to provide the compound **11** (108 mg, 17% yield) as white powder.

^{1}H NMR (500 MHz, DMSO) δ 1.12–1.91 (br, 24H), 4.02–4.07 (m, 1H), 7.42 (d, J = 9.00 Hz, 2H), 7.84 (d, J = 9.00 Hz, 2H), 8.76 (br, 1H), 9.25 (s, 1H); ^{13}C NMR (125 MHz, $CDCl_3$) δ 22.1 (2C), 22.7 (2C), 26.0 (2C), 37.2 (2C), 42.5 (2C), 42.9 (2C), 43.6, 52.7 (2C), 120.9 (2C), 129.3 (2C), 130.4, 135.0, 157.6, 158.8; HRMS (ESI), *m/z* calcd for $C_{23}H_{33}ClN_3O_2$ (MH^+) 418.2256, found 418.2261.

4.1.9. N^1-(4-Chlorophenyl)-N^2-(4-fluorophenyl)oxalamide (14)

To a solution of the ethyl 2-((4-chlorophenyl)amino)-2-oxoacetate (1.21 g, 5.00 mmol) in EtOH (25.0 mL) were added Et_3N (1.38 mL, 10.0 mmol) and 4-fluoroaniline **12** (1.44 mL, 15.0 mmol). The reaction mixture was stirred for 3 h at 150 °C under microwave irradiation. After being cooled to room temperature, the crystal was collected and washed with cold EtOH and *n*-hexane, and dried under reduced pressure to provide the compound **14** (601 mg, 41% yield) as colorless crystals. Compounds **15** and **16** were similarly synthesized.

^{1}H NMR (500 MHz, $CDCl_3$) δ 7.07–7.14 (m, 2H), 7.35–7.40 (m, 2H), 7.59–7.63 (m, 4H), 9.29 (s, 1H), 9.33 (s, 1H); ^{13}C NMR (125 MHz, DMSO) δ 115.8 (d, J = 22.5 Hz, 2C), 122.5 (2C), 122.8 (d, J = 7.5 Hz, 2C), 128.8, 129.1 (2C), 134.4, 137.1, 158.3, 158.9 (d, J = 42.5 Hz), 160.2; HRMS (ESI), *m/z* calcd for $C_{14}H_{11}ClFN_2O_2$ (MH^+) 293.0488, found 293.0485.

4.1.10. N^1-(4-Chlorophenyl)-N^2-(2-(pyridin-2-yl)ethyl) oxalamide (17)

To a solution of the ethyl 2-((4-chlorophenyl)amino)-2-oxoacetate (726.3 mg, 3.00 mmol) in EtOH (10.0 mL) were added Et_3N (0.831 mL, 6.00 mmol) and 2-(pyridin-2-yl)ethanamine 14 (1.07 mL, 9.00 mmol). The reaction mixture was stirred for 3 h at 150 °C under microwave irradiation. After being cooled to room temperature, the crystal was collected and washed with cold EtOH and *n*-hexane, and dried under reduced pressure to provide the title compound **17** (336 mg, 37% yield) as colorless crystals.

^{1}H NMR (500 MHz, $CDCl_3$) δ 3.08 (t, J = 6.50 Hz, 2H), 3.82 (q, J = 6.50 Hz, 2H), 7.12–7.21 (m, 2H), 7.30–7.37 (m, 2H),7.54–7.66 (m 3H), 8.40 (s, 1H), 8.60 (d, J = 5.00 Hz, 1H), 9.26 (s, 1H); ^{13}C NMR (125 MHz, $CDCl_3$) δ 36.5, 39.0, 121.0 (2C), 121.8, 123.4, 129.2 (2C), 130.3, 135.1, 136.7, 149.5, 157.5, 158.6, 159.6; HRMS (ESI), *m/z* calcd for $C_{15}H_{15}ClN_3O_2$ (MH^+) 304.0847, found 304.0850.

4.2. Molecular modeling

The structures of compounds **11** and **12** were built in Sybyl and minimized with the MMFF94 force field and partial charges.[17] Dockings were then performed using FlexSIS through its SYBYL module, into the crystal structure of gp120 (PDB: 1RZJ).

4.3. FACS analysis

JR-FL (R5, Sub B) chronically infected PM1 cells were pre-incubated with 100 μM of a CD4 mimic for 15 min, and then incubated with an anti-HIV-1 mAb, 4C11, at 4 °C for 15 min. The cells were washed with PBS, and fluorescein isothiocyanate (FITC)-conjugated goat anti-human IgG antibody was used for antibody-staining. Flow cytometry data for the binding of 4C11 (green lines, Fig. 4) to the Env-expressing cell surface in the presence of a CD4 mimic are shown among gated PM1 cells along with a control antibody (anti-human CD19: black lines, Fig. 4). Data are representative of the results from a minimum of two independent experiments. The number at the bottom of each graph in Figure 4 shows the mean fluorescence intensity (MFI) of the antibody 4C11.

Acknowledgments

This work was supported in part by Grant-in-Aid for Scientific Research from the Ministry of Education, Culture, Sports, Science, and Technology of Japan, and Health and Labour Sciences Research Grants from Japanese Ministry of Health, Labor, and Welfare.

Supplementary data

Supplementary data (NMR charts of compounds) associated with this article can be found, in the online version, at doi:10.1016/j.bmc.2011.09.045.

References and notes

1. Selected reviews of the drug developments targeting HIV entry process: (a) Blair, W. S.; Lin, P. F.; Meanwell, N. A.; Wallace, O. B. *Drug Discovery Today* **2000**, *5*, 183; (b) D'Souza, M. P.; Cairns, J. S.; Plaeger, S. F. *J. Am. Med. Assoc.* **2000**, *284*, 215; (c) Labranche, C. C.; Galasso, G.; Moore, J. P.; Bolognesi, D.; Hirsch, M. S.; Hammer, S. M. *Antivir. Res.* **2001**, *50*, 95; (d) Pierson, T. C.; Doms, R. W. *Immunol. Lett.* **2003**, *85*, 113; (e) Tamamura, H.; Otaka, A.; Fujii, N. *Curr. HIV Res.* **2005**, *3*, 289.
2. Chan, D. C.; Kim, P. S. *Cell* **1998**, *93*, 681.
3. (a) Alkhatib, G.; Combadiere, C.; Broder, C. C.; Feng, Y.; Kennedy, P. E.; Murphy, P. M.; Berger, E. A. *Science* **1996**, *272*, 1955; (b) Choe, H.; Farzan, M.; Sun, Y.; Sullivan, N.; Rollins, B.; Ponath, P. D.; Wu, L.; Mackay, C. R.; LaRosa, G.; Newman, W.; Gerard, N.; Gerard, C.; Sodroski, J. *Cell* **1996**, *85*, 1135; (c) Deng, H. K.; Liu, R.; Ellmeier, W.; Choe, S.; Unutmaz, D.; Burkhart, M.; Marzio, P. D.; Marmon, S.; Sutton, R. E.; Hill, C. M.; Davis, C. B.; Peiper, S. C.; Schall, T. J.; Littman, D. R.; Landau, N. R. *Nature* **1996**, *381*, 661; (d) Doranz, B. J.; Rucker, J.; Yi, Y. J.; Smyth, R. J.; Samson, M.; Peiper, S. C.; Parmentier, M.; Collman, R. G.; Doms, R. W. *Cell* **1996**, *85*, 1149; (e) Dragic, T.; Litwin, V.; Allaway, G. P.; Martin, S. R.; Huang, Y.; Nagashima, K. A.; Cayanan, C.; Maddon, P. J.; Koup, R. A.; Moore, J. P.; Paxton, W. A. *Nature* **1996**, *381*, 667.
4. Feng, Y.; Broder, C. C.; Kennedy, P. E.; Berger, E. A. *Science* **1996**, *272*, 872.
5. (a) Briz, V.; Poveda, E.; Soriano, V. *J. Antimicrob. Chemother.* **2006**, *57*, 619; (b) Rusconi, S.; Scozzafava, A.; Mastrolorenzo, A.; Supuran, C. T. *Curr. Drug Targets Infect. Disord.* **2004**, *4*, 339; (c) Shaheen, F.; Collman, R. G. *Curr. Opin. Infect. Dis.* **2004**, *17*, 7; (d) Markovic, I. *Curr. Pharm. Des.* **2006**, *12*, 1105.
6. Zhao, Q.; Ma, L.; Jiang, S.; Lu, H.; Liu, S.; He, Y.; Strick, N.; Neamati, N.; Debnath, A. K. *Virology* **2005**, *339*, 213.
7. (a) Kwong, P. D.; Wyatt, R.; Robinson, J.; Sweet, R. W.; Sodroski, J.; Hendrickson, W. A. *Nature* **1998**, *393*, 648; (b) Kwong, P. D.; Wyatt, R.; Mcajeed, S.; Robinson, J.; Sweet, R. W.; Sodroski, J.; Hendrickson, W. A. *Structure* **2000**, *8*, 1329.

8. Schön, A.; Madani, N.; Klein, J. C.; Hubicki, A.; Ng, D.; Yang, X.; Smith, A. B., III; Sodroski, J.; Freire, E. *Biochemistry* **2006**, *45*, 10973.
9. Yoshimura, K.; Harada, S.; Shibata, J.; Hatada, M.; Yamada, Y.; Ochiai, C.; Tamamura, H.; Matsushita, S. *J. Virol.* **2010**, *84*, 7558.
10. Madani, N.; Schön, A.; Princiotto, A. M.; LaLonde, J. M.; Courter, J. R.; Soeta, T.; Ng, D.; Wang, L.; Brower, E. T.; Xiang, S.-H.; Do Kwon, Y.; Huang, C.-C.; Wyatt, R.; Kwong, P. D.; Freire, E.; Smith, A. B., III; Sodroski, J. *Structure* **2008**, *16*, 1689.
11. Yamada, Y.; Ochiai, C.; Yoshimura, K.; Tanaka, T.; Ohashi, N.; Narumi, T.; Nomura, W.; Harada, S.; Matsushita, S.; Tamamura, H. *Bioorg. Med. Chem. Lett.* **2010**, *20*, 354.
12. Narumi, T.; Ochiai, C.; Yoshimura, K.; Harada, S.; Tanaka, T.; Nomura, W.; Arai, H.; Ozaki, T.; Ohashi, N.; Matsushita, S.; Tamamura, H. *Bioorg. Med. Chem. Lett.* **2010**, *20*, 5853.
13. LaLonde, J. M.; Elban, M. A.; Courter, J. R.; Sugawara, A.; Soeta, T.; Madani, N.; Princiotto, A. M.; Kwon, Y. D.; Kwong, P. D.; Schön, A.; Freire, E.; Sodroski, J.; Smith, A. B., III *Bioorg. Med. Chem. Lett.* **2011**, *20*, 354.
14. Olofson, R. A.; Abbott, D. E. *J. Org. Chem.* **1984**, *49*, 2795.
15. Sakai, K.; Yamada, K.; Yamasaki, T.; Kinoshita, Y.; Mito, F.; Utsumi, H. *Tetrahedron* **2010**, *66*, 2311.
16. Bordwell, F. G.; Ji, G. Z. *J. Am. Chem. Soc.* **1991**, *113*, 8398.
17. Halgren, T. A. *J. Comput. Chem.* **1996**, *17*, 490.